

# Epitaxial Mn<sub>5</sub>Ge<sub>3</sub> nano-islands on a Ge(001) surface

Howon Kim<sup>1</sup>, Goo-Eun Jung<sup>1</sup>, Jin-Hyung Lim<sup>1</sup>,  
Kyung Hoon Chung<sup>1</sup>, Se-Jong Kahng<sup>1</sup>, Won-joon Son<sup>2</sup> and  
Seungwu Han<sup>3</sup>

<sup>1</sup> Department of Physics, Korea University, 1-5, Anam-dong, Seongbuk-gu, Seoul 136-713, Korea

<sup>2</sup> School of Chemistry, Seoul National University, Seoul 151-742, Korea

<sup>3</sup> Department of Physics, Ewha Womans University, Seoul 120-750, Korea

E-mail: [sjkahng@korea.ac.kr](mailto:sjkahng@korea.ac.kr)

Received 11 August 2007, in final form 12 October 2007

Published 6 December 2007

Online at [stacks.iop.org/Nano/19/025707](http://stacks.iop.org/Nano/19/025707)

## Abstract

The growth behavior and atomic structure of Mn germanide, grown on Ge(001), is studied with x-ray diffraction and scanning probe microscopy. The amorphous clusters of as-deposited Mn are crystallized into Mn<sub>5</sub>Ge<sub>3</sub> nano-islands with a size of ~100 nm by solid phase epitaxy. At low coverage, the shape of the nano-islands is plateau-like, while at increased coverage it becomes mound-like. At the flat top of the plateau-like nano-islands, the hexagonal atomic structure is resolved. It is interpreted, with the help of first-principles study, as a Mn-terminated Mn<sub>5</sub>Ge<sub>3</sub>(0001) structure.

(Some figures in this article are in colour only in the electronic version)

## 1. Introduction

Controlled injection of spin polarized electrons into a semiconductor is crucial for the implementation of semiconductor-based spintronics, which aims at utilizing the spin degree of freedom in future electronic devices [1]. Efforts have been made to grow specific semiconductors with magnetic properties, or to design the appropriate heterostructures of magnetic metals and semiconductors. A promising system in this field is Mn–Ge on Ge substrates. Their fabrication processes are beneficially compatible with conventional Si technology. It has been reported that Mn can work as a dilute impurity, making Ge magnetic [2–4]. The rough consensus is that Mn germanides are likely to grow during the growth process of Mn–Ge alloy [2–12]. It was recently pointed out that the growth of Mn germanide, especially Mn<sub>5</sub>Ge<sub>3</sub>, is in fact quite valuable; it is a magnetic metal which can be used in the form of heterostructures due to its sufficiently high Curie temperature [13–16]. The growth structure in such heterostructures is an essential element in determining the efficiency of spin polarized injection. Experimental studies on Ge(111) regarding solid phase epitaxy [13, 14] have been reported, but are still lacking on Ge(001). This (001) surface is more practical for

electronic devices than the (111) surface in Ge and Si, due to their abundant electronic states in that direction.

In this paper, we report the growth behavior and atomic structures of Mn germanide on Ge(001), studied with x-ray diffraction (XRD), atomic force microscopy (AFM) and scanning tunneling microscopy (STM). Similar to Ge(111), it is observed that Mn<sub>5</sub>Ge<sub>3</sub> nano-islands grow on Ge(001) during solid phase epitaxy. With increased coverage, the shape as well as the height of nano-islands undergoes transition, from plateau-like to mound-like. Atomic structure at the top of the plateau-like island is resolved in STM images, and compared with the result of first-principles study.

## 2. Experiment

The growth experiments were carried out in our ultrahigh-vacuum (UHV) system with a base pressure of  $3 \times 10^{-11}$  Torr. XRD and AFM experiments were done *ex situ*, while the STM experiment was done *in situ* using a home-built STM [17]. (001)-oriented, Sb-doped, n-type germanium substrates were prepared by repeated cycles of 500 eV Ne<sup>+</sup> sputtering and annealing at 1000 K for ~20 min. Surface cleanliness was checked by the STM images of reconstructed Ge(001) (figure 1(a), inset). Mn was deposited by using a Knudsen

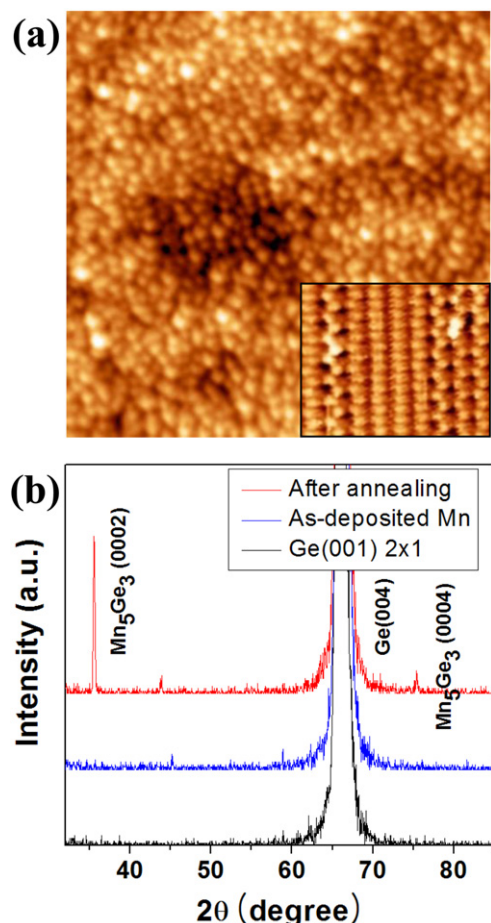


**Figure 1.** (a) STM image of as-deposited Mn on a clean Ge(001) surface, 130 nm  $\times$  130 nm. Tunneling current was 0.3 nA. Sample bias was  $-1.4$  V. Inset: STM image of Ge(001) surface with  $p(2 \times 1)$  and  $c(4 \times 2)$  reconstructions. (b) Three x-ray diffraction  $\theta$ - $2\theta$  spectra obtained from a bare Ge(001) surface (bottom), as-deposited 45 ML Mn at room temperature (middle), after annealing at  $\sim 700$  K for 20 min (top).

cell on the Ge(001) at room temperature, and subsequently annealed at 700–800 K for  $\sim 20$  min. The growth rate could be adjusted around 3 monolayers (ML)  $\text{min}^{-1}$ , as determined with a quartz thickness monitor and STM images. The STM images were obtained in the constant-current mode with a PtRh tip.

### 3. Result and discussion

When Mn was deposited at room temperature on Ge(001), no ordered surface structure was found. Figure 1(a) shows a typical STM image of as-deposited Mn on Ge(001) at  $\sim 15$  ML. Mn forms clusters of several nanometers in size, due to limited surface diffusion. XRD analysis was performed in order to figure out the crystallinity of as-deposited Mn. Figure 1(b) shows three XRD  $\theta$ - $2\theta$  spectra, obtained from a bare Ge(001), as-deposited Mn on Ge(001), and annealed Mn on Ge(001). The spectrum from as-deposited Mn on Ge(001) shows generally the same trend as that from the bare Ge(001). They show a strong peak at  $\theta = 65.95^\circ$ , the (004)  $hkl$  reflection peak of Ge(001). This suggests that the clusters of as-deposited

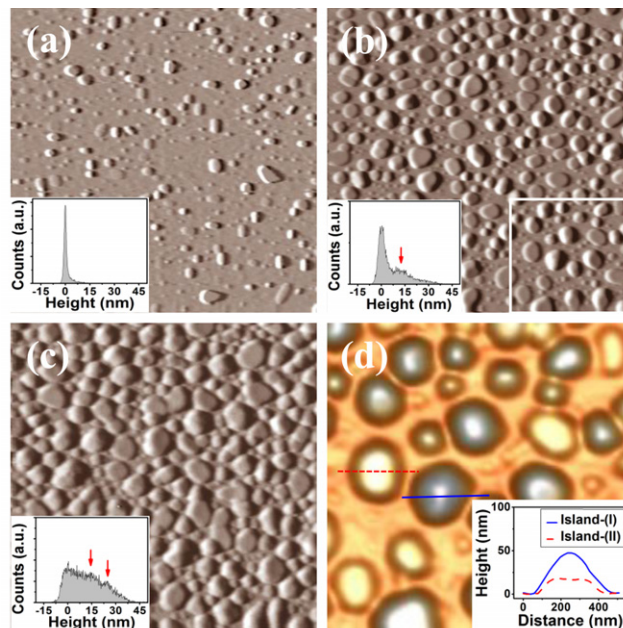


**Figure 2.** 5  $\mu\text{m} \times 5 \mu\text{m}$  AFM images obtained from three samples after annealing at  $\sim 700$  K for 20 min, with different coverages of Mn: (a) 5 ML, (b) 15 ML and (c) 45 ML. Insets in (a), (b) and (c) are the height distributions of the each sample. The (red) arrows denote peak positions. They correspond to the most probable height for the nano-islands. (d) Three-dimensionally zoomed AFM image of the rectangular area in (b). The inset in (d) shows height profiles along the (red) dotted line and (blue) solid line in this image.

Mn, observed in STM images, are most likely amorphous rather than crystalline. The XRD spectrum, from annealed Mn on Ge(001), shows an additional strong peak at  $\theta = 35.54^\circ$ . It is assigned as the  $\text{Mn}_5\text{Ge}_3(0002)$  reflection. A higher-order reflection of  $\text{Mn}_5\text{Ge}_3(0004)$  is also visible in the spectrum at  $\theta = 75.44^\circ$ . Our observations advocate the stoichiometric relation that the surface of  $\text{Mn}_5\text{Ge}_3(0001)$  is parallel with that of Ge(001), which is consistent with the reports from the embedded  $\text{Mn}_5\text{Ge}_3$  precipitates using transmission electron microscopy [7–9]. There is a weak peak at  $\theta = 45^\circ$ , which possibly comes from  $\text{Mn}_{11}\text{Ge}_8(270)$ , but this will never form the majority in our sample.

The surface morphology of grown systems after annealing was studied with AFM. Figure 2 shows the AFM images, obtained at three different coverages, 5, 15 and 45 ML. A common feature observed in AFM images is three-dimensional islands. As the coverage is increased, the density of the islands increases. It is inferred that the three-dimensional islands will be the  $\text{Mn}_5\text{Ge}_3$  structures observed in our XRD analysis. With increased coverage, it was observed that the lateral sizes of islands increase up to several hundred nanometers. We call these three-dimensional islands nano-islands. The height distributions of the nano-islands are visualized in the insets of figure 2, where the brightness of the AFM images is analyzed. At 5 ML, the height distribution is relatively narrow and dominated by the substrate surface, due to the small number of islands. As coverage is increased, the distribution becomes wider and wider. It is also discovered that there is one peak at 15 ML, and two peaks at 45 ML, as noted by the arrows in

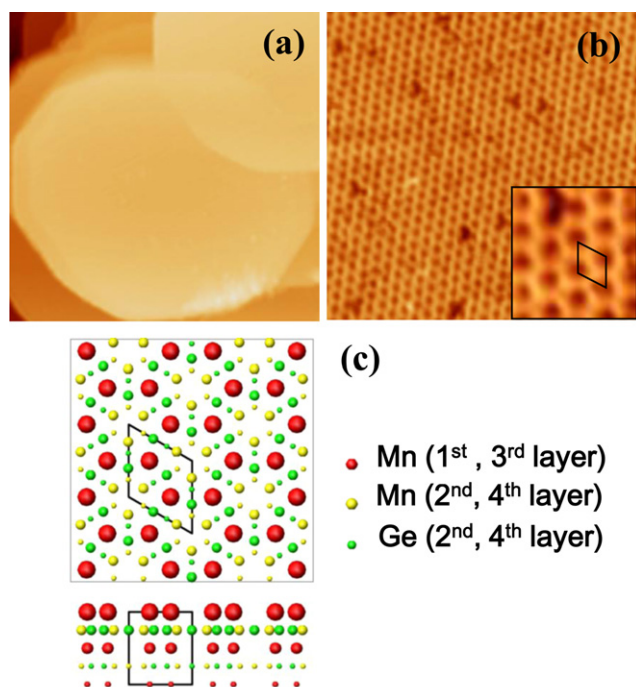


**Figure 3.** STM images obtained from the top-most surface of plateau-like  $\text{Mn}_5\text{Ge}_3$  nano-islands. The image sizes are (a)  $120\text{ nm} \times 120\text{ nm}$  and (b)  $14\text{ nm} \times 14\text{ nm}$ . Sample bias  $-1.3\text{ V}$ . Tunneling current: (a)  $0.3\text{ nA}$  and (b)  $0.2\text{ nA}$ . (c) Atomic ball model for the  $\text{Mn}_5\text{Ge}_3$  crystal structure. Top view (upper) and side view (bottom). The rhombus in the model represents the lattice unit cell. In the side view four layers form a unit cell. The first and third layers are identical Mn-only layers. The second and fourth layers are mixed MnGe layers with mirror-reflection symmetry between them.

the insets of figures 2(b) and (c), respectively. This suggests that there exist two kinds of nano-islands with two different heights. Figure 2(d) shows a three-dimensionally zoomed image of the area marked in figure 2(b). It is obvious that

there are two different kinds of nano-island in the image. Cross sections are taken, as shown in the inset of figure 2(d), from two representative nano-islands. The height profiles reveal that not only their heights but also that their shapes show striking contrast. The tall one (Island-I) is about twice as high as the short one (Island-II). The tall one shows a mound-like shape with a sharp peak, while the short one shows a plateau-like shape with a flat top. It seems that the plateau-like short islands grow in the early stage, followed by the growth of mound-like tall islands. A possible reason for this shape evolution can be elastic strain. For example, mound-like islands may be more favorable in strain relaxation at above a certain size than plateau-like ones. Since the AFM and XRD measurements were performed *ex situ*, there can be oxides on the surface. However, atomic diffusion and reaction is limited at room temperature. Oxide structure will be small compared to the nano-islands, and will not distort the results of AFM and XRD.

High-resolution atomic images were obtained from plateau-like islands with STM. Figures 3(a) and (b) show typical step and atomic resolution images. In the atomic-level images, hexagonal symmetry is clearly resolved. This observation can be accounted for by the  $\text{Mn}_5\text{Ge}_3(0001)$  structure. It was reported that the surface of  $\text{Mn}_5\text{Ge}_3(0001)$  could be either Mn-terminated or Mn-Ge alloy-terminated [13–15]. An atomic ball model for the Mn-terminated case is presented in figure 3(c). On the Mn-terminated surface, it is expected that the first-layer Mn atoms will constitute the surface morphology, revealing a hexagonal honeycomb structure. In order to confirm this speculation, a first-principles study has been made.

To simulate STM images of the  $\text{Mn}_5\text{Ge}_3(0001)$  surfaces we use the computational code Vienna *Ab initio* Simulation Package (VASP) [18]. The interactions between electrons and ions are described by projector-augmented-wave (PAW) potentials [19] and the exchange and correlation energies of electrons are described within the spin polarized generalized

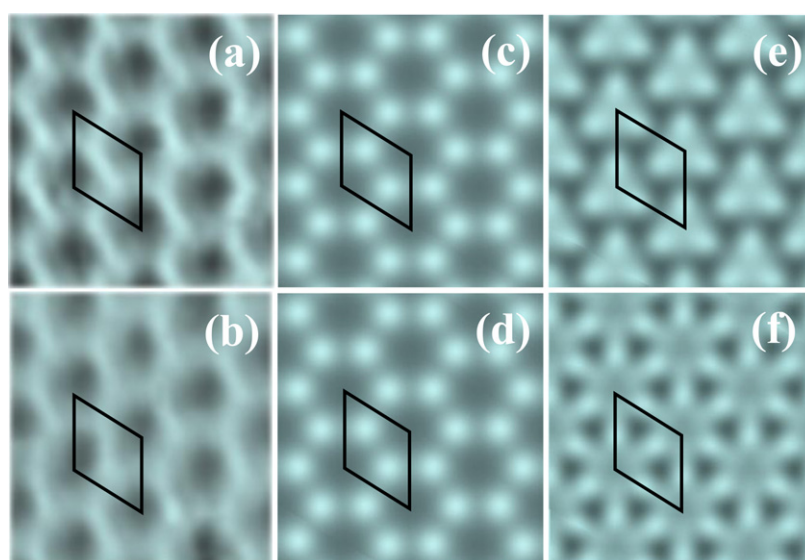


**Figure 4.** STM images obtained experimentally at the sample bias of (a)  $-1.2\text{ V}$  and (b)  $+1.2\text{ V}$ . Simulated STM images for Mn-terminated  $\text{Mn}_5\text{Ge}_3(0001)$  at the sample bias of (c)  $-1.2\text{ V}$  and (d)  $+1.2\text{ V}$ . Simulated STM images for mixed MnGe-terminated  $\text{Mn}_5\text{Ge}_3(0001)$  at the sample bias of (e)  $-1.2\text{ V}$  and (f)  $+1.2\text{ V}$ . The rhombus in all the images represents the lattice unit cell.

gradient approximation with a functional form proposed in [20]. The plane waves with an energy cutoff of 300 eV are used for expanding electronic wavefunctions. For the  $k$ -point integration,  $4 \times 4$  regular meshes are used for the surface unit cell. The density of states is broadened with a width of 0.2 eV and the atomic positions are relaxed until the Hellmann–Feynman force on each atom is reduced to within  $0.025 \text{ eV \AA}^{-1}$ . The STM images are simulated based on the Tersoff–Hamann approximation [21].

In figure 4, experimentally observed STM images are presented in (a) and (b) with opposite polarity, and simulated images are in (c)–(f). The set of (c) and (d) is from the Mn-terminated surface, while the set of (e) and (f) is from the mixed MnGe-terminated surface. The images in (a)–(d) basically show the honeycomb ordering. Atomic structure in the filled state is almost the same as that in the empty state, in experimental images as well as simulated images. On the other hand, the simulated images from mixed MnGe-terminated surfaces do not show honeycomb structure but show a more complicated structure than those from Mn-terminated surfaces. They cannot match to experimental observation, and the possibility of mixed MnGe-terminated  $\text{Mn}_5\text{Ge}_3(0001)$  is ruled out. The observed surface is therefore Mn-terminated  $\text{Mn}_5\text{Ge}_3(0001)$ , similar to the case grown on Ge(111) [13, 14]. When a Mn atom in the first layer is missing, then the defect will tend to show an atomic depression. Since the surface structure is of a honeycomb shape, it is natural that the depression will be Y-shaped. Such Y-shaped depressions are often found in our STM images (figure 3(b)).

Concerning the surface stoichiometry, it is observed that the  $\text{Mn}_5\text{Ge}_3[\bar{2}110]$  direction is parallel to the Ge[110] direction, the dimer row direction of the Ge surface in our STM image [22]. The lattice mismatch in this direction is 3.4%. On the Ge(111) surface, similarly, the  $\text{Mn}_5\text{Ge}_3[\bar{2}110]$  direction is parallel to Ge[110]. The alignment between  $\text{Mn}_5\text{Ge}_3[\bar{2}110]$  and Ge[110] is strongly preferred in both surfaces. On the other hand, the surface direction of  $\text{Mn}_5\text{Ge}_3(0001)$  is parallel to the surface directions of both surfaces, namely a different crystallographic alignment. According to transmission electron microscopy,  $\text{Mn}_5\text{Ge}_3(0001)$  grows in parallel to Ge(001) in embedded  $\text{Mn}_5\text{Ge}_3$  precipitates, which is in good agreement with our observation [7–9]. It was pointed out that the lattice mismatch (11%) between successive lattice planes of  $\text{Mn}_5\text{Ge}_3(0001)$  and Ge(001) is smaller than the lattice mismatch (29%) between lattice planes of  $\text{Mn}_5\text{Ge}_3(0001)$  and Ge(111), and that the former is preferred.

We were unable to resolve the atomic structure of mound-like islands. In many cases, crystalline structures (if there is any) are more stable than amorphous ones. As we have annealed the sample for a long enough time, amorphous structure must be transformed to crystalline structures. It is conceived that mound-like islands will be crystalline with similar stoichiometry to plateau-like ones.

#### 4. Summary

In summary, the atomic structure of Mn germanide grown on Ge(001) was studied. We observed that  $\text{Mn}_5\text{Ge}_3$  grows in the

form of nano-islands. The shape of the nano-islands shows an evolution from a plateau-like to a mound-like shape. Atomic structure with hexagonal symmetry was observed in STM images and explained with Mn-terminated  $\text{Mn}_5\text{Ge}_3(0001)$  structure.

#### Acknowledgments

The authors acknowledge financial support by the Korean Government (MOEHRD, MOST), through the Korea Research Foundation (Basic Research Promotion Fund, KRF-2003-015-C00208 and KRF-2004-005-C00060), and through the Korea Science and Engineering Foundation (KOSEF, R01-2007-000-11545-0 and M10503000187-05M0300-18710). HK acknowledges a Seoul Science Fellowship from the Seoul City Government for graduate student funding.

#### References

- [1] Timm C 2003 *J. Phys.: Condens. Matter* **15** R1865
- [2] Park Y D, Wilson A, Hanbicki A T, Matteson J E, Ambrose T, Spanos G and Jonker B T 2001 *Appl. Phys. Lett.* **78** 2739
- [3] Cho S, Choi S, Hong S C, Kim Y, Ketterson J B, Kim B-J, Kim Y C and Jung J-H 2002 *Phys. Rev. B* **66** 033303
- [4] Li A P, Shen J, Thompson J R and Weitering H H 2005 *Appl. Phys. Lett.* **86** 152507
- [5] Li A P, Wendelken J F, Shen J, Feldman L C, Thompson J R and Weitering H H 2005 *Phys. Rev. B* **72** 195205
- [6] Ottaviano L, Passacantando M, Picozzi S, Continenza A, Gunnella R, Verna A, Impellizzeri G and Priolo F 2006 *Appl. Phys. Lett.* **88** 061907
- [7] Passacantando M, Ottaviano L, D’Orazio F, Lucari F, De Biase M, Impellizzeri G and Priolo F 2006 *Phys. Rev. B* **73** 195207
- [8] Verna A et al 2006 *Phys. Rev. B* **74** 085204
- [9] Bihler C, Jaeger C, Vallaitis T, Gjukic M, Brandt M S, Pippel E, Woltersdorf J and Gosele U 2006 *Appl. Phys. Lett.* **88** 112506
- [10] Chen J, Wang K L and Galatsis K 2007 *Appl. Phys. Lett.* **90** 012510
- [11] Kim S-K, Cho Y C, Jeong S-Y, Cho C-R, Park S E, Lee J H, Kim J-P, Kim Y C and Choi H W 2007 *Appl. Phys. Lett.* **90** 192505
- [12] Kim S K, Park S E, Cho Y C, Cho C R and Jeong S-Y 2006 *J. Korean Phys. Soc.* **49** s518
- [13] Zeng C, Erwin S C, Feldman L C, Li A P, Jin R, Song Y, Thompson J R and Weitering H H 2003 *Appl. Phys. Lett.* **83** 5002
- [14] Zeng C, Zhu W, Erwin S C, Zhang Z and Weitering H H 2004 *Phys. Rev. B* **70** 205340
- [15] Picozzi S, Continenza A and Freeman A J 2004 *Phys. Rev. B* **70** 235205
- [16] Zhu W, Weitering H H, Wang E G, Kaxiras E and Zhang Z 2004 *Phys. Rev. Lett.* **93** 126102
- [17] Kim S T 2006 *Ms Thesis* Korea University
- [18] Kresse G and Hafner J 1993 *Phys. Rev. B* **47** 558(R)
- [18] Kresse G and Hafner J 1994 *Phys. Rev. B* **49** 14251
- [19] Blöchl P E 1994 *Phys. Rev. B* **50** 17953
- [20] Perdew J P, Burke K and Ernzerhof M 1996 *Phys. Rev. Lett.* **77** 3865
- [21] Tersoff J and Hamann D R 1985 *Phys. Rev. B* **31** 805
- [22] Kim H et al 2007 *Surf. Sci.* at press